

Semiclassical description of quantum coherence effects and their quenching: A forward–backward initial value representation study

Haobin Wang, Michael Thoss,^{a)} Kathy L. Sorge, Ricard Gelabert, Xavier Giménez,^{b)} and William H. Miller^{c)}

Department of Chemistry, University of California, and Chemical Sciences Division, Lawrence Berkeley National Laboratory, Berkeley, California 94720

(Received 18 September 2000; accepted 13 November 2000)

The forward–backward (FB) version of the semiclassical (SC) initial value representation (IVR) is used to study quantum coherence effects in the time-dependent probability distribution of an anharmonic vibrational coordinate and its quenching when coupled to a thermal bath. It is shown that the FB-IVR accurately reproduces the detailed quantum coherent structure in the weak coupling regime, and also describes how this coherence is quenched with an increase of the system–bath coupling and/or the bath temperature. Comparisons are made with other approximations and the physical implications are discussed. © 2001 American Institute of Physics.

[DOI: 10.1063/1.1337802]

I. INTRODUCTION

An accurate description of quantum effects in polyatomic molecular system is a challenging task in chemical reaction dynamics. Though considerable progress has been made in the recent years on rigorous quantum-mechanical methods,¹ they are at present only applicable to relatively small molecular systems. One is thus necessarily interested in developing and applying useful approximations to treat more complex systems, i.e., those with many degrees of freedom. Semiclassical (SC) initial value representations (IVR),² provide an approximate way of including quantum effects into classical molecular-dynamics (MD) simulations, and are currently undergoing a rebirth of interest in this regard.^{3–13} A number of recent applications^{3–13} have shown the SC-IVR to be of good accuracy for a wide variety of phenomena. The primary remaining challenge is to make SC-IVR approaches practical enough for application to complex molecular systems.

Essentially all dynamical quantities of interest in a complex molecular system can be expressed in terms of a time correlation function of the form¹⁴

$$C_{AB}(t) = \text{tr}[\hat{A} e^{i\hat{H}t/\hbar} \hat{B} e^{-i\hat{H}t/\hbar}], \quad (1.1)$$

operator \hat{A} typically involves the Boltzmann operator of the complete molecular system, and \hat{B} often only a few (perhaps collective) variables. A semiclassical approximation for $C_{AB}(t)$ can be obtained by using the IVR for the time evolution operator $e^{-i\hat{H}t/\hbar}$, the Herman–Kluk³ or coherent state version of which is given by

$$e^{-i\hat{H}t/\hbar} = (2\pi\hbar)^{-N} \int d\mathbf{q}_0 \int d\mathbf{p}_0 C_t(\mathbf{p}_0, \mathbf{q}_0) e^{iS_t(\mathbf{p}_0, \mathbf{q}_0)/\hbar} \times |\mathbf{p}_t \mathbf{q}_t\rangle \langle \mathbf{p}_0 \mathbf{q}_0|, \quad (1.2)$$

where N is the number of degrees of freedom, $(\mathbf{p}_0, \mathbf{q}_0)$ are initial momenta and coordinates for classical trajectories, $\mathbf{p}_t = \mathbf{p}_t(\mathbf{p}_0, \mathbf{q}_0)$ and $\mathbf{q}_t = \mathbf{q}_t(\mathbf{p}_0, \mathbf{q}_0)$ are the classically time-evolved phase space variables, $S_t(\mathbf{p}_0, \mathbf{q}_0)$ is the classical action integral along the trajectory, and $C_t(\mathbf{p}_0, \mathbf{q}_0)$ is the pre-exponential factor determined by the following combination of the monodromy matrix elements:

$$C_t(\mathbf{p}_0, \mathbf{q}_0) = \sqrt{\det \left[\frac{1}{2} \left(\gamma^{1/2} \frac{\partial \mathbf{q}_t}{\partial \mathbf{q}_0} \gamma^{-1/2} + \gamma^{-1/2} \frac{\partial \mathbf{p}_t}{\partial \mathbf{p}_0} \gamma^{1/2} - i\hbar \gamma^{1/2} \frac{\partial \mathbf{q}_t}{\partial \mathbf{p}_0} \gamma^{1/2} + \frac{i}{\hbar} \gamma^{-1/2} \frac{\partial \mathbf{p}_t}{\partial \mathbf{q}_0} \gamma^{-1/2} \right) \right]}. \quad (1.3)$$

In the above expression γ denotes a N -dimensional diagonal matrix, with element γ_i being the width parameter for the

coherent state of the i th degree of freedom. The coordinate space representation of an N -dimensional coherent state is the product of N one-dimensional minimum uncertainty wave packets

$$\langle \mathbf{x} | \mathbf{p} \mathbf{q} \rangle = \prod_{i=1}^N \left(\frac{\gamma_i}{\pi} \right)^{1/4} e^{-\left(\gamma_i/2 \right) (x_i - q_i)^2 + (i/\hbar) p_i (x_i - q_i)}. \quad (1.4)$$

^{a)}Present address: Theoretische Chemie, Technische Universität München, Lichtenbergstr. 4, 85747 Garching, Germany.

^{b)}On sabbatical leave from Departament de Química Física, Universitat de Barcelona. Martí i Franqués, 1, 08028 Barcelona, Spain.

^{c)}Electronic mail: miller@neon.chem.berkeley.edu

Since the Heisenberg time evolution in Eq. (1.1) involves two time evolution operators, use of the IVR for the propagators, Eq. (1.2), leads to the following *double* phase space average for the time correlation function

$$C_{AB}(t) = (2\pi\hbar)^{-2N} \int d\mathbf{q}_0 \int d\mathbf{p}_0 \int d\mathbf{q}'_0 \int d\mathbf{p}'_0 \\ \times C_i^*(\mathbf{p}'_0, \mathbf{q}'_0) C_i(\mathbf{p}_0, \mathbf{q}_0) e^{i[S_i(\mathbf{p}_0, \mathbf{q}_0) - S_i(\mathbf{p}'_0, \mathbf{q}'_0)]/\hbar} \\ \times \langle \mathbf{p}_0 \mathbf{q}_0 | \hat{A} | \mathbf{p}'_0 \mathbf{q}'_0 \rangle \langle \mathbf{p}'_0 \mathbf{q}'_0 | \hat{B} | \mathbf{p}_t \mathbf{q}_t \rangle. \quad (1.5)$$

The practical difficulty with the above formulation is that the integrand in the double phase space average is highly oscillatory and amplified by pre-exponential factors $C_i(\mathbf{p}_0, \mathbf{q}_0)$ and $C_i(\mathbf{p}'_0, \mathbf{q}'_0)$ that can become large. To sidestep this problem, a linearized approximation to the SC-IVR expression in Eq. (1.5), the LSC-IVR, was introduced,¹⁵ whereby all the relevant quantities in the integrand are expanded to first order in the difference variables $\mathbf{p}_0 - \mathbf{p}'_0$ and $\mathbf{q}_0 - \mathbf{q}'_0$. The integration over these difference variables can be carried out analytically, which yields the following much simpler classical-looking expression for the correlation function, for Eq. (1.1):

$$C_{AB}(t) = (2\pi\hbar)^{-N} \int d\mathbf{q}_0 \int d\mathbf{p}_0 A^w(\mathbf{p}_0, \mathbf{q}_0) B^w(\mathbf{p}_t, \mathbf{q}_t), \quad (1.6)$$

where A^w and B^w are the Wigner transforms of operators \hat{A} and \hat{B} . That is, this linearization of the SC-IVR leads to the ‘‘classical Wigner’’ model that has arisen before from a variety of different approaches.¹⁶ Application of this approximation to several interesting condensed phase problems^{15,17} was quite successful; it is in general good for short time and has, therefore, been useful in defining an approximate quantum version of transition state theory¹⁸ (for which C_{AB} is the flux-flux autocorrelation function¹⁹). A more thorough analysis,²⁰ however, showed that the LSC-IVR is incapable of describing quantum coherence effects in the longer time dynamics. This motivated the development of the *forward-backward* (FB) IVR²¹ that goes beyond the linearized approximation, yet is still more efficient than evaluating Eq. (1.5).

The FB-IVR approach²¹ for time correlation functions utilizes an idea introduced by Makri and Thompson for numerical evaluation of influence functionals in path integral calculations,²² namely to combine the forward and backward time evolution operators into *one* semiclassical time propagation. In the FB-IVR, the operator product $e^{i\hat{H}t/\hbar} \hat{B} e^{-i\hat{H}t/\hbar}$ in Eq. (1.1) is represented by a *single* Herman-Kluk-type IVR, i.e., Eq. (1.2), where the trajectories evolve from time $0 \rightarrow t$ (the action of the operator $e^{-i\hat{H}t/\hbar}$), undergo momenta and/or coordinates jumps at time t (the effect of operator \hat{B}), and then evolve backward from $t \rightarrow 0$ (the action of operator $e^{i\hat{H}t/\hbar}$). The benefit gained from the FB-IVR, besides reducing the dimensionality of the phase space integral, is that there is a partial cancellation of the phase of the integrand and the magnitude of the pre-exponential factor, thus greatly improving the numerical properties of the integrand. Application of the FB-IVR to several problems—femtosecond

photoelectron spectroscopy of I_2^- ,⁹ molecular energy transfer,⁹ thermal rate constant calculation using flux correlation function,²³ and diffraction through a two-slit coupled to a thermal bath²⁴—have shown that it is capable of describing quantum coherence effects quite accurately.

In this paper we apply the FB-IVR to the study of a generic vibrational relaxation process of a diatomic molecule coupled to a cluster or condensed phase environment, modeled here as a bath of harmonic modes. These processes, which are of fundamental importance for many chemical reactions in solution, have been intensively studied in the recent years, both experimentally and theoretically (for some recent reviews see, for example, Refs. 25–28). Many of these investigations have focused on the calculation or measurement of vibrational relaxation rates. With the availability of ultrafast spectroscopy techniques, however, more specific dynamical information can be obtained (see, for example, Refs. 29–32). Within this context, the question of the observability of quantum coherence and interference effects in a complex system is of interest. In this article, we will study the extent to which quantum coherence/interference structure, present in the wave-packet dynamics of an isolated diatomic molecule, is quenched when the molecule is coupled to a thermal environment.

The quantity of interest for this purpose is the time-dependent density for a vibrational coordinate s coupled to a thermal bath

$$P_t(r) = \frac{1}{Q_B} \text{tr}[e^{-\beta\hat{H}_B} |\Phi_0\rangle \langle \Phi_0| e^{i\hat{H}_t/\hbar} \delta(s-r) e^{-i\hat{H}_t/\hbar}], \quad (1.7)$$

where $|\Phi_0\rangle$ is the initial state for the vibrational coordinate, and H_B is the Hamiltonian for the thermal bath with partition function Q_B ; note that $P_t(r)$ is the correlation function of Eq. (1.1) with $\hat{A} = e^{-\beta\hat{H}_B} |\Phi_0\rangle \langle \Phi_0|$ and $\hat{B} = \delta(s-r)$. The structure of $P_t(r)$ can reveal (*vide infra*) time-dependent information of quantum coherence for the vibrational coordinate s .

The purpose of the present work is to investigate the generic character of quantum coherence effects in the probability distribution function $P_t(r)$ and the extent to which this is quenched by a bath in various parameter regimes. We will discuss in some detail the accuracy of classical MD simulations which are widely used to study such processes. Section II summarizes the FB-IVR approach for calculating time correlation functions, and Sec. III gives the specifics of our model and the calculational procedure. Section IV presents the results obtained via FB-IVR and their comparisons with other methods. Section V summarizes and concludes.

II. SUMMARY OF THEORY

In order to cast the correlation function $C_{AB}(t)$, Eq. (1.1), into the form for the FB-IVR, operator \hat{B} must first be written in exponential form. If \hat{B} is a local function (more general operators can also be treated²¹) of the single variable $s(\mathbf{q})$, which itself may be a function of many of the dynamical coordinates \mathbf{q} , then this is accomplished by Fourier transform, i.e.,

$$\hat{B} \equiv B[s(\hat{\mathbf{q}})] = \int_{-\infty}^{\infty} dp_s \tilde{B}(p_s) e^{ip_s s(\hat{\mathbf{q}})/\hbar}, \quad (2.1a)$$

where $\tilde{B}(p_s)$ is the Fourier transform of $B(s)$

$$\tilde{B}(p_s) = \frac{1}{2\pi\hbar} \int_{-\infty}^{\infty} ds e^{-ip_s s/\hbar} B(s). \quad (2.1b)$$

For example, for $B(s) = \delta(s-r)$ as in Eq. (1.7), one has

$$\tilde{B}(p_s) = \frac{1}{2\pi\hbar} e^{-ip_s r/\hbar}. \quad (2.2)$$

The correlation function Eq. (1.1) then becomes

$$C_{AB}(t) = \int_{-\infty}^{\infty} dp_s \tilde{B}(p_s) \text{tr}[\hat{A} \hat{U}(t)], \quad (2.3a)$$

where

$$\hat{U}(t) = e^{i\hat{H}t/\hbar} e^{ip_s s(\mathbf{q})/\hbar} e^{-i\hat{H}t/\hbar}. \quad (2.3b)$$

The three operators in Eq. (2.3b) describe, sequentially from right to left, propagation from 0 to t , a momentum jump at time t , and then propagation from t back to 0. The Herman–Kluk IVR for operator $\hat{U}(t)$ thus has the same form as Eq. (1.2), so that the FB-IVR for the correlation function is

$$C_{AB}(t) = \int_{-\infty}^{\infty} dp_s \tilde{B}(p_s) (2\pi\hbar)^{-N} \int d\mathbf{p}_0 \int d\mathbf{q}_0 \\ \times \langle \mathbf{p}_0 \mathbf{q}_0 | \hat{A} | \mathbf{p}'_0 \mathbf{q}'_0 \rangle C_0(\mathbf{p}_0, \mathbf{q}_0; p_s) e^{iS_0(\mathbf{p}_0, \mathbf{q}_0; p_s)/\hbar}. \quad (2.4)$$

The FB-IVR trajectory involved in Eq. (2.4) begins at $t=0$ with initial condition $(\mathbf{p}_0, \mathbf{q}_0)$ and evolves to time t under the molecular Hamiltonian H ; at time t the momentum is changed according to

$$\mathbf{p}_t \rightarrow \mathbf{p}_t + p_s \left[\frac{\partial s(\mathbf{q})}{\partial \mathbf{q}} \right]_{\mathbf{q}=\mathbf{q}_t}, \quad (2.5)$$

and the trajectory is then evolved back to time 0 via the molecular Hamiltonian H , $(\mathbf{p}'_0, \mathbf{q}'_0)$ being the final phase point. The action integral S_0 has contributions from these three time steps

$$S_0(\mathbf{p}_0, \mathbf{q}_0; p_s) = \int_0^t d\tau [\mathbf{p}_\tau \cdot \dot{\mathbf{q}}_\tau - H] + p_s s(\mathbf{q}_t) \\ + \int_t^0 d\tau [\mathbf{p}'_\tau \cdot \dot{\mathbf{q}}'_\tau - H], \quad (2.6)$$

and the pre-exponential factor $C_0(\mathbf{p}_0, \mathbf{q}_0)$ has the same form as Eq. (1.3)

$$C_0(\mathbf{p}_0, \mathbf{q}_0; p_s) = \sqrt{\det \left[\frac{1}{2} \left(\gamma^{1/2} \frac{\partial \mathbf{q}'_0}{\partial \mathbf{q}_0} \gamma^{-1/2} + \gamma^{-1/2} \frac{\partial \mathbf{p}'_0}{\partial \mathbf{p}_0} \gamma^{1/2} - i\hbar \gamma^{1/2} \frac{\partial \mathbf{q}'_0}{\partial \mathbf{p}_0} \gamma^{1/2} + \frac{i}{\hbar} \gamma^{-1/2} \frac{\partial \mathbf{p}'_0}{\partial \mathbf{q}_0} \gamma^{-1/2} \right) \right]}. \quad (2.7)$$

At time t when the momentum jump occurs, Eq. (2.5), the monodromy matrix (used to calculate the pre-exponential factor) is changed according to²⁴

$$\frac{\partial \mathbf{p}_t}{\partial \mathbf{p}_0} \rightarrow \frac{\partial \mathbf{p}_t}{\partial \mathbf{p}_0}, \quad \frac{\partial \mathbf{p}_t}{\partial \mathbf{q}_0} \rightarrow \frac{\partial \mathbf{p}_t}{\partial \mathbf{q}_0} + p_s \frac{\partial^2 s(\mathbf{q}_t)}{\partial \mathbf{q}_t^2}, \quad (2.8)$$

$$\frac{\partial \mathbf{q}_t}{\partial \mathbf{p}_0} \rightarrow \frac{\partial \mathbf{q}_t}{\partial \mathbf{p}_0}, \quad \frac{\partial \mathbf{q}_t}{\partial \mathbf{q}_0} \rightarrow \frac{\partial \mathbf{q}_t}{\partial \mathbf{q}_0}.$$

It is clear that if $s(\mathbf{q})$ is a linear function of \mathbf{q} , then the monodromy matrix remains the same during the momentum jump.

The forward–backward nature of the trajectory induces, to a great extent, partial cancellation of the phase in the integrand, thus making the calculation much more feasible for complex systems. In situations where operator \hat{B} only depends on a few collective coordinates (which is typically the case for dynamical calculations of complex systems), there are only a few more integrals than the (single) classical

phase space integral. Therefore, the FB-IVR provides one of the simplest ways to capture quantum effects via classical MD simulations.

III. DETAILS OF THE CALCULATION

This section defines the specific model we use to study coherence effects (and their quenching) in the time-dependent density of a vibrational coordinate, Eq. (1.7). Specifics of the FB-IVR calculation are also discussed.

A. The model

We consider a single vibrational degree of freedom (which can either describe the vibration of a diatomic molecule or a collective coordinate) coupled to a thermal bath, representing the environment (e.g., a cluster, a liquid, a surface, a protein, etc.). The thermal bath is modeled by a collection of harmonic oscillators, each linearly coupled to the vibrational coordinate. The total Hamiltonian is thus given by

$$H = H_s(p, s) + \sum_{j=1}^{N_b} \left[\frac{1}{2} P_j^2 + \frac{1}{2} \omega_j^2 \left(Q_j + \frac{c_j}{\omega_j^2} (s - s_e) \right)^2 \right], \quad (3.1a)$$

$$H_s(p, s) = \frac{1}{2m} p^2 + V(s), \quad (3.1b)$$

where s and p are coordinate and momentum of the vibrational degree of freedom, respectively, and $\{Q_i, P_i\}$ are the mass-scaled coordinates and momenta for the bath. A Morse potential is used for the vibrational coordinate

$$V(s) = D_e [1 - e^{-\alpha(s-s_e)}]^2, \quad (3.2)$$

where $m = 1.165 \times 10^5$ a.u. (reduced mass), $D_e = 1.2547 \times 10^4 \text{ cm}^{-1}$, $s_e = 2.6663 \text{ \AA}$, and $\alpha = 1.8576 \text{ \AA}^{-1}$, which correspond to the ground-state potential of molecular I_2 .³³ The essential property of the harmonic bath is its spectral density³⁴

$$J(\omega) = \frac{\pi}{2} \sum_j \frac{c_j^2}{\omega_j} \delta(\omega - \omega_j), \quad (3.3)$$

which is chosen in the Ohmic form with an exponential cut-off

$$J_o(\omega) = \eta \omega e^{-\omega/\omega_c}. \quad (3.4)$$

Here ω_c is the characteristic frequency of the bath, which is chosen as $\omega_c = 20 \text{ cm}^{-1}$. η is the coupling strength between the bath and the vibrational coordinate, and is varied in this paper in order to investigate the effect of the bath on the coherence of the vibrational motion.

The continuous bath spectral density of Eq. (3.4) can be discretized to the form of Eq. (3.3) via the relation

$$c_j^2 = \frac{2}{\pi} \omega_j \frac{J_o(\omega_j)}{\rho(\omega_j)}, \quad (3.5)$$

where $\rho(\omega)$ is a density of frequencies satisfying

$$\int_0^{\omega_j} d\omega \rho(\omega) = j, \quad j = 1, \dots, N_b, \quad (3.6a)$$

here chosen as

$$\rho(\omega) = a \frac{J_o(\omega)}{\omega}, \quad (3.6b)$$

with

$$a = \frac{N_b}{\eta \omega_c} \frac{1}{1 - e^{-\omega_m/\omega_c}}, \quad (3.6c)$$

where ω_m is the largest frequency of the bath modes considered in the calculation. With the above scheme of discretization, we found that 20–40 modes with $\omega_m = 5 \omega_c$ is adequate to describe the continuous spectral density for the parameters considered in this paper.

B. FB-IVR for $P_t(r)$

The FB-IVR expression for $P_t(r)$, Eq. (1.7), is straightforwardly obtained by applying the procedure described in the previous section for the general time correlation function. It is given by (hereafter we set $\hbar = 1$)

$$P_t(r) = \frac{1}{Q_B} \frac{1}{2\pi} \int_{-\infty}^{\infty} dp_s e^{-ip_s r} \frac{1}{(2\pi)^{N_B+1}} \int d\mathbf{p}_0 \int d\mathbf{q}_0 \\ \times C_0(\mathbf{p}_0, \mathbf{q}_0; p_s) e^{iS_0(\mathbf{p}_0, \mathbf{q}_0; p_s)} \\ \times \langle \mathbf{p}_0 \mathbf{q}_0 | e^{-\beta \hat{H}_B} | \Phi_0 \rangle \langle \Phi_0 | \mathbf{p}'_0 \mathbf{q}'_0 \rangle. \quad (3.7)$$

The initial wave function for the s -degree of freedom is chosen as a coherent state

$$\langle s | \Phi_0 \rangle = \left(\frac{\gamma_o}{\pi} \right)^{1/4} e^{-(\gamma_o/2)(s-q_i)^2} e^{ip_i(s-q_i)}, \quad (3.8)$$

where q_i and p_i denote the average position and momentum of the initial wave packet, and γ_o is the width parameter of the coherent state. In this work $p_i = 0$, $q_i = 2.4 \text{ \AA}$, and $\gamma_o = m \omega_s$ are used, where ω_s is the harmonic frequency of the Morse oscillator

$$\omega_s = \alpha \sqrt{2D_e/m} \approx 213.7 \text{ cm}^{-1}. \quad (3.9)$$

Coherent state matrix elements of various operators are straightforward

$$\langle \mathbf{p}_0 \mathbf{q}_0 | \hat{A} | \mathbf{p}'_0 \mathbf{q}'_0 \rangle = \langle p_0 s_0 | \Phi_0 \rangle \langle \Phi_0 | p'_0 s'_0 \rangle \\ \times \prod_{j=1}^{N_B} \langle P_{j0} Q_{j0} | e^{-\beta \hat{H}_{Bj}} | P'_{j0} Q'_{j0} \rangle, \quad (3.10a)$$

$$\langle p_0 s_0 | \Phi_0 \rangle = e^{-(\gamma_s/4)(s_o - q_i)^2} e^{-(1/4\gamma_s)(p_o - p_i)^2} e^{(i/2)(p_o + p_i)(s_o - q_i)}, \quad (3.10b)$$

$$\langle p_{j0} q_{j0} | e^{-\beta \hat{H}_{bj}} | p'_{j0} q'_{j0} \rangle = e^{-u_j} e^{-(\gamma_j/4)(q_{j0}^2 + q'_{j0}{}^2)} e^{-(1/4\gamma_j)(p_{j0}^2 + p'_{j0}{}^2)} e^{(i/2)(p_{j0} q_{j0} - p'_{j0} q'_{j0})} \\ \times \exp \left\{ \frac{1}{2} e^{-2u_j} \left[\gamma_j q_{j0} q'_{j0} + \frac{1}{\gamma_j} p_{j0} p'_{j0} + i(p'_{j0} q_{j0} - p_{j0} q'_{j0}) \right] \right\}, \quad (3.10c)$$

where $u_j = \beta \omega_j / 2$, and the width parameters of the FB-IVR coherent states are chosen as

$$\gamma_s = \gamma_0 = m \omega_s, \quad \gamma_j = \omega_j. \quad (3.11)$$

C. Initial condition and time propagation

In the present work, the sampling function of initial phase space variables $\{\mathbf{p}_0, \mathbf{q}_0\}$ is taken as

$$W(\mathbf{p}_0, \mathbf{q}_0) = \frac{1}{D} |\langle p_0 s_0 | \Phi_0 \rangle| \prod_j \langle p_{j0} q_{j0} | e^{-\beta \hat{H}_{bj}} | p_{j0} q_{j0} \rangle, \quad (3.12a)$$

where D is the proper normalization factor, and $\langle p_{j0} q_{j0} | e^{-\beta \hat{H}_{bj}} | p_{j0} q_{j0} \rangle$ is the diagonal part of Eq. (3.10c), i.e., the Husimi distribution³⁵ for the bath Boltzmann operator

$$\begin{aligned} &\langle p_{j0}q_{j0}|e^{-\beta\hat{H}_{bj}}|p_{j0}q_{j0}\rangle \\ &= e^{-u_j} \exp\left[-\frac{\gamma_j}{2}(1-e^{-2u_j})q_{j0}^2 - \frac{1}{2\gamma_j}(1-e^{-2u_j})p_{j0}^2\right]. \end{aligned} \tag{3.12b}$$

One may also use the Husimi distribution $|\langle p_{0s0}|\Phi_0\rangle|^2$ for the s -degree of freedom so that $W(\mathbf{p}_0, \mathbf{q}_0)$ is the Husimi distribution for the overall system.²³ This, however, turns out to be less efficient for the present application.

For the additional integration over the momentum jump variable, p_s , the integrand is oscillatory. However, this is a one-dimensional Fourier transform, which is easily carried out by a standard quadrature.

Time propagations of the phase space variables and the monodromy matrix (including the momentum jump) follow the standard procedure for classical equations of motion. Reference 23 gives the specifics and some variants in this regard, so they will not be repeated here. On the other hand, we would like to discuss a few useful technical points which have not been mentioned previously.

The first technical point is related to the action integral, which is defined in differential form as

$$\dot{S}_t = \mathbf{p}_t \cdot \dot{\mathbf{q}}_t - H, \tag{3.13}$$

i.e., the time derivative of S_t has a magnitude similar to the total energy, which can be large for a complex system. In a mass-weighted Cartesian coordinate system with Hamiltonian

$$H = \frac{\mathbf{p}^2}{2} + V(\mathbf{q}), \tag{3.14}$$

a new quantity ϕ_t can be integrated instead of S_t ,

$$\phi_t = S_t + \frac{1}{2}(\mathbf{p}_0 \cdot \mathbf{q}_0 - \mathbf{p}_t \cdot \mathbf{q}_t), \tag{3.15}$$

with the initial condition $\phi_0 = 0$ and time derivative given by

$$\dot{\phi}_t = \frac{1}{2} \frac{\partial V}{\partial \mathbf{q}_t} \cdot \mathbf{q}_t - V(\mathbf{q}_t). \tag{3.16}$$

It is easy to see that $\dot{\phi}_t = 0$ for a harmonic system. For a general anharmonic system, all the second-order terms in the Hamiltonian disappear [thus no kinetic-energy terms appear in Eq. (3.16)]. Specifically, for the present Hamiltonian, Eq. (3.1), $\dot{\phi}_t$ is given by

$$\begin{aligned} \dot{\phi}_t &= \frac{1}{2} \frac{\partial V(s_t)}{\partial s_t} s_t - V(s_t) + \frac{1}{2} \sum_j \frac{c_j^2}{\omega_j^2} s_e (s_t - s_e) \\ &\quad + \frac{1}{2} \sum_j c_j Q_j s_e, \end{aligned} \tag{3.17}$$

where $V(s)$ is the Morse potential of Eq. (3.2). It is obvious that ϕ_t varies much more slowly than S_t .

For the FB-IVR approach of the present problem, this new variable ϕ has three parts, that are similar to Eq. (2.6),

$$\begin{aligned} \phi_0(\mathbf{p}_0, \mathbf{q}_0; p_s) &= \int_0^t d\tau [\mathbf{p}_\tau \cdot \dot{\mathbf{q}}_\tau - H] + \frac{1}{2}(\mathbf{p}_0 \cdot \mathbf{q}_0 - \mathbf{p}'_0 \cdot \mathbf{q}'_0) \\ &\quad + p_s s_t + \int_t^0 d\tau [\mathbf{p}'_\tau \cdot \dot{\mathbf{q}}'_\tau - H] \\ &= \int_0^t d\tau [\mathbf{p}_\tau \cdot \dot{\mathbf{q}}_\tau - H] + \frac{1}{2}(\mathbf{p}_0 \cdot \mathbf{q}_0 - \mathbf{p}_t \cdot \mathbf{q}_t) \\ &\quad + \frac{1}{2} p_s s_t + \frac{1}{2}(\mathbf{p}'_t \cdot \mathbf{q}'_t - \mathbf{p}'_0 \cdot \mathbf{q}'_0) \\ &\quad + \int_t^0 d\tau [\mathbf{p}'_\tau \cdot \dot{\mathbf{q}}'_\tau - H] \\ &= \int_0^t d\tau \left[\frac{1}{2} \frac{\partial V}{\partial \mathbf{q}_\tau} \cdot \mathbf{q}_\tau - V(\mathbf{q}_\tau) \right] + \frac{1}{2} p_s s_t \\ &\quad + \int_t^0 d\tau \left[\frac{1}{2} \frac{\partial V}{\partial \mathbf{q}'_\tau} \cdot \mathbf{q}'_\tau - V(\mathbf{q}'_\tau) \right], \end{aligned} \tag{3.18}$$

where the integrand is given in Eq. (3.17). In the above expression, the extra term besides the action integral, $\frac{1}{2}(\mathbf{p}_0 \cdot \mathbf{q}_0 - \mathbf{p}'_0 \cdot \mathbf{q}'_0)$, is actually present in the coherent state matrix elements in Eq. (3.10). Therefore, not only is ϕ easier to integrate, but it also incorporates terms in the FB-IVR phase so that they need not be collected in the final expression.

The next technical point is related to the evaluation of the pre-exponential factor C_t , Eqs. (1.3) and (2.7), where the square root of a complex quantity needs to be evaluated. The standard way of keeping track of the correct branch of the square root is to evaluate C_t at sufficiently small time intervals to make sure that it is continuous. This, however, becomes increasingly more difficult as the number of degrees of freedom increases, which can be understood from analysis of a system consisting of N -harmonic oscillators

$$H = \sum_{j=1}^N \left(\frac{1}{2} P_j^2 + \frac{1}{2} \omega_j^2 Q_j^2 \right). \tag{3.19}$$

If the width parameters of the coherent states are chosen as $\gamma_j = \omega_j$, it is easy to show that Eq. (1.3) gives

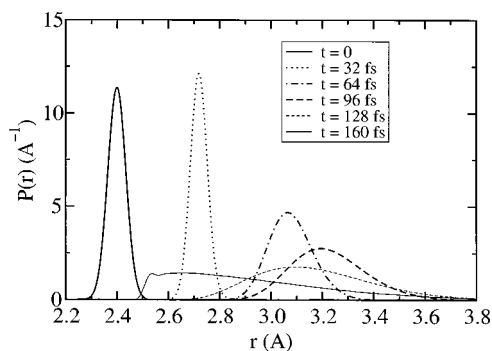
$$C_t^2 = \exp\left(-it \sum_{j=1}^N \omega_j\right). \tag{3.20a}$$

The correct value of the square-root is of course

$$C_t = \exp\left(-it \sum_{j=1}^N \omega_j / 2\right), \tag{3.20b}$$

but numerically tracking the correct branch of the square root would require a very small time interval for many degrees of freedom. In fact, for a system consisting many degrees of freedom (such as considered in this paper), the usual way of tracking the phase requires a time interval that is smaller than the propagation time step. On the other hand, if C_t is re-expressed as

$$C_t = \exp\left(-it \sum_{j=1}^N \omega_j / 2\right) D_t, \tag{3.21a}$$

FIG. 1. $P_t(r)$ for the one-dimensional vibration at short time.

where D_t is defined by

$$D_t = \sqrt{C_t^2 \exp\left(it \sum_{j=1}^N \omega_j\right)}, \quad (3.21b)$$

then the phase of D_t is much easier to track.

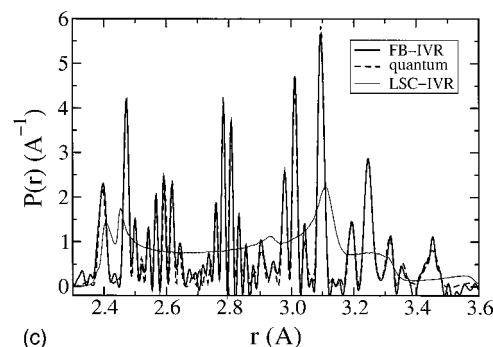
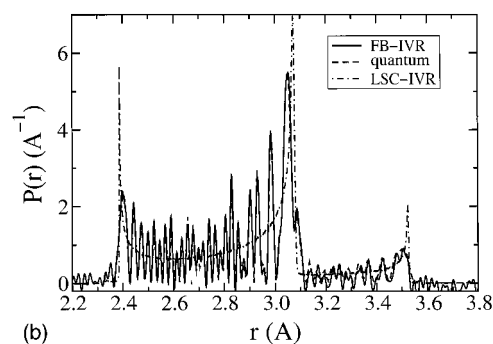
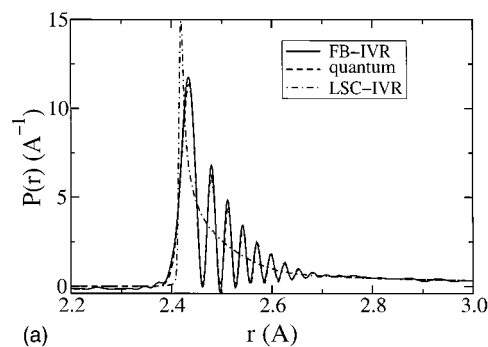
For harmonic systems, $D_t = 1$, so its phase need not be tracked at all. For a general anharmonic system, one can define D_t , Eq. (3.21b), using the normal mode frequencies so that the major part of the phase of C_t is canceled before taking the square root. Our tests show that by utilizing Eq. (3.21), the time interval needed to keep the phase of C_t continuous can be quite large, and it is rather insensitive to an increase in the number of degrees of freedom.

IV. RESULTS AND DISCUSSION

A. One-dimensional vibration

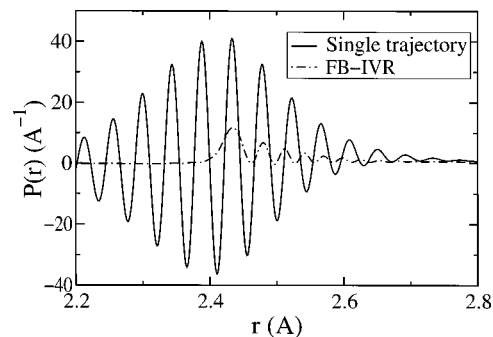
To access the accuracy of the FB-IVR and various other approximations, we first investigate the behavior of $P_t(r)$ for the one-dimensional Morse oscillator, where comparisons can be made with the exact quantum mechanical result. Figure 1 shows $P_t(r)$ within approximately the first vibrational period (the harmonic vibrational period is ~ 156 fs for the present parameter set of I_2), obtained via the FB-IVR. As described in the previous section, the initial coherent state, $|\Phi_0\rangle = |p_i, q_i\rangle, p_i = 0, q_i = 2.4 \text{ \AA}$ is placed left to the equilibrium position of the Morse oscillator, $s_e = 2.6663 \text{ \AA}$, i.e., the oscillator is initially compressed. At $t = 0$, the wave function starts traveling to the right until reaching the first turning point, then returning to the left. Since the potential is anharmonic, $P_t(r)$ does not retain the Gaussian form as time increases. However, within the first vibrational period, the structure of the density $P_t(r)$ is fairly simple and can be well approximated by the LSC-IVR.

Figure 2(a) shows $P_t(r)$ at $t = 192$ fs, i.e., right after the first vibrational period. At this time very prominent quantum coherent structure appears. Compared with the exact quantum-mechanical result, the FB-IVR does an excellent job in reproducing all the detailed coherent structure, whereas the LSC-IVR completely misses it. More impressive results are shown in Figs. 2(b) and 2(c), for $t = 640$ fs and $t = 1600$ fs, respectively, where even more complicated coherent structure is developed. Though this structure seems ‘‘noisy,’’ it represents true quantum interference effects, as seen from the excellent agreement between the FB-IVR and

FIG. 2. $P_t(r)$ for the one-dimensional vibration at longer time: (a) $t = 192$ fs; (b) $t = 640$ fs; (c) $t = 1600$ fs.

the exact quantum results. The LSC-IVR/classical Wigner model, on the other hand, fails to capture such interference/coherence, which is expected from previous studies.²⁰

In the above calculation, 50 000–100 000 trajectories are needed in order to achieve numerical convergence. Another semiclassical approximation, which is widely used in dy-

FIG. 3. Comparison of $P_t(r)$ obtained from the single trajectory calculation and the FB-IVR for the one-dimensional vibration at $t = 192$ fs.

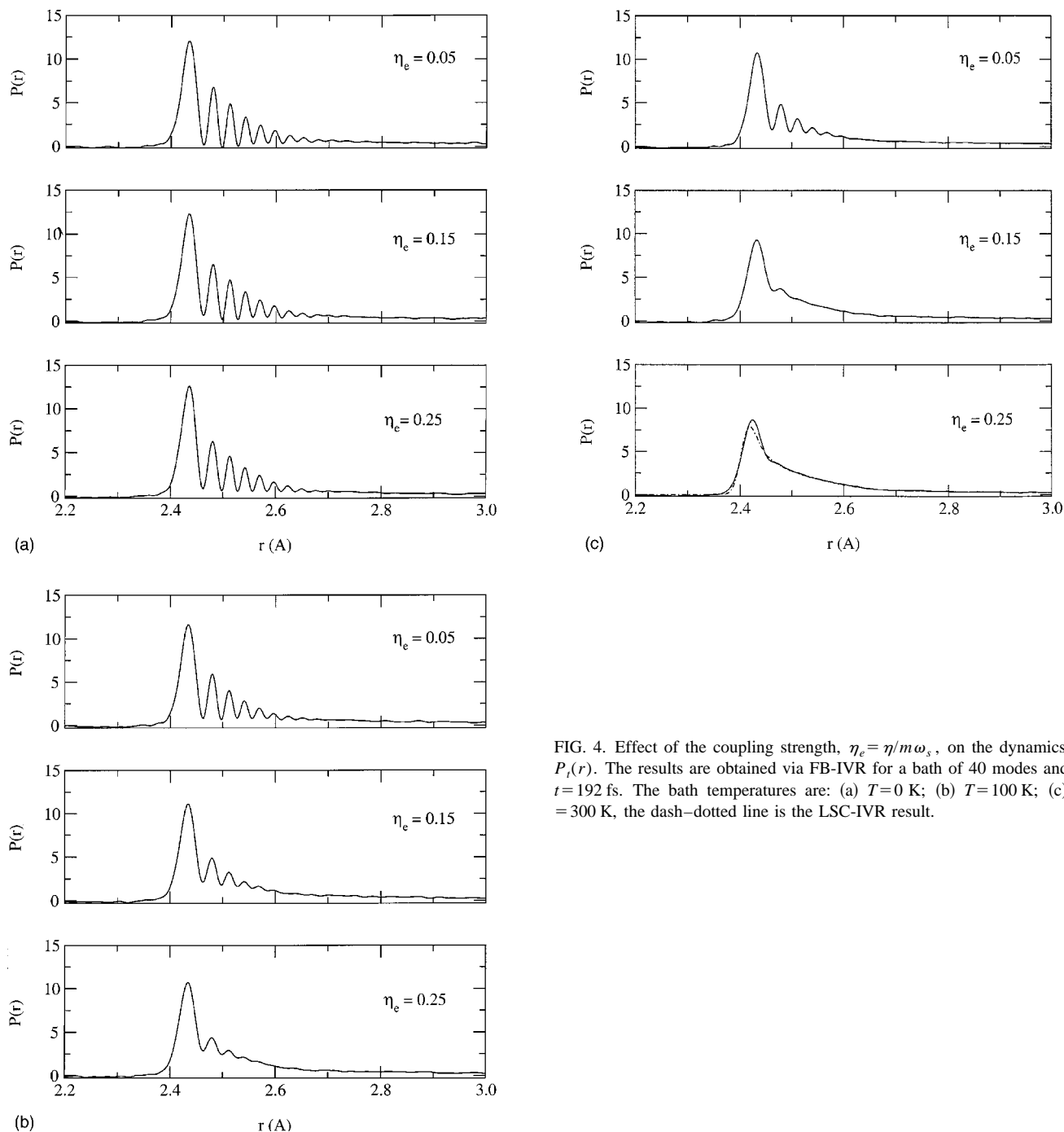


FIG. 4. Effect of the coupling strength, $\eta_e = \eta/m\omega_s$, on the dynamics of $P_t(r)$. The results are obtained via FB-IVR for a bath of 40 modes and at $t=192$ fs. The bath temperatures are: (a) $T=0$ K; (b) $T=100$ K; (c) $T=300$ K, the dash-dotted line is the LSC-IVR result.

namical simulations for complex systems, is the *single trajectory approximation*. In this approach, one (or a few that can represent the initial wave function) frozen Gaussian is propagated via classical mechanics, instead of carrying out the complete phase space integral $(2\pi)^{-1} \int dp_0 \int dq_0$. The initial conditions of the classical trajectory, (p_0, q_0) , are set to the corresponding average values obtained from the initial wave function, e.g., for the present case

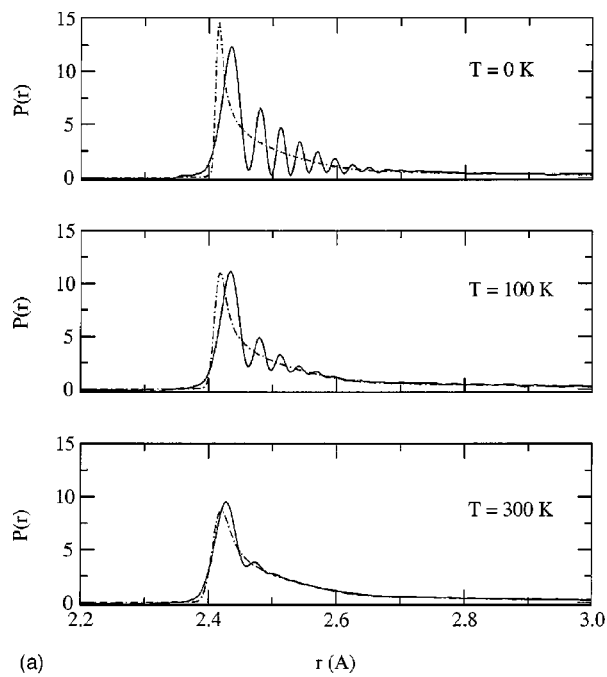
$$p_0 = p_i, \quad q_0 = q_i. \quad (4.1)$$

Unlike the LSC-IVR/classical Wigner model, this approximation often exaggerates the coherence. Applying it in the context of the FB-IVR causes even more serious problems, as shown in Fig. 3. The result obtained from this approxima-

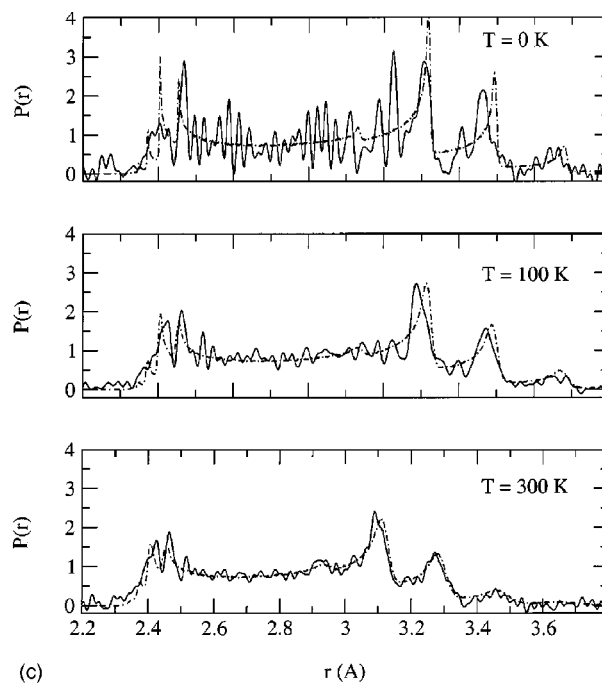
tion not only introduces more spurious coherent peaks, but also makes a large part of $P_t(r)$ negative, which is clearly unphysical. Thus caution must be taken in interpreting the results obtained from such single trajectory calculations. The structure they show may not be true quantum coherence phenomena.

B. Vibrational relaxation in the presence of a thermal bath

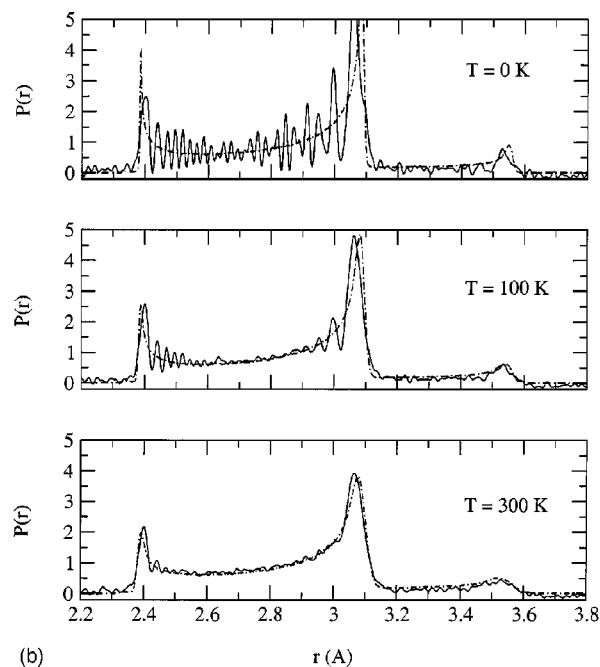
The coherent structure of the molecular vibration, which will persist for infinitely long time if the molecule is isolated, will however, be quenched if the vibrational coordinate is coupled to a thermal bath. The extent of this quenching is



(a)



(c)



(b)

FIG. 5. Effect of the bath temperature on the dynamics of $P_t(r)$. The results are obtained via the FB-IVR (solid line) and the LSC-IVR (dashed-dotted line) for a bath of 40 modes, with the coupling strength $\eta_e = \eta/m\omega_s = 0.15$. (a) $t = 192$ fs; (b) $t = 640$ fs; (c) $t = 1600$ fs.

investigated here as a function of the bath temperature and the coupling strength between the vibrational coordinate and the bath.

Figure 4 shows the effect of the system-bath coupling strength on $P_t(r)$ for $t = 192$ fs, obtained via the FB-IVR approach. Figure 4(a) is for zero bath temperature, where almost all the coherent structure of $P_t(r)$ for the previous one-dimensional vibration is retained, though slightly quenched at a stronger coupling strength. The effect of the coupling strength on $P_t(r)$ is more profound at $T = 100$ K, Fig. 4(b), where a coherent to incoherent transition is observed as the effective coupling strength $\eta_e = \eta/m\omega_s$ increases. This temperature is still too low, however, to induce complete decoherence, and quantum effects are still quite

evident. Figure 4(c) shows $P_t(r)$ at $T = 300$ K, where the temperature is sufficiently high that at strong coupling, $\eta_e = 0.25$, all the coherent structure disappears. The LSC-IVR/classical Wigner model is in good agreement with the FB-IVR result at this classical decoherent limit.

Figure 5 illustrates the effect of the bath temperature on $P_t(r)$, at $\eta_e = 0.15$. The transition from coherent to incoherent behavior is apparent as temperature increases. At lower temperatures, there is appreciable quantum coherence/interference even with a reasonably large system-bath coupling ($\eta_e = 0.15$), which is consistent with the general observation that quantum effects are important for low temperatures. Decoherence is achieved at $T = 300$ K, where

the FB-IVR results can be well approximated by the LSC-IVR/classical Wigner model. In this regime, classical mechanics is adequate in describing the dynamics of a complex system.

For all the examples considered above, 50 000–100 000 trajectories are sufficient to reach numerical convergences for the longest time (1600 fs), and fewer trajectories are needed for shorter times. One may note that this number of trajectories for 41 degrees of freedom is the same as for a one-dimensional Morse oscillator presented in the previous section. Indeed, we have found that the forward–backward nature of the trajectories make the integrand much smoother than the usual double phase space average, and thus the number of trajectories is rather insensitive to the increase in the number of degrees of freedom. This property of the FB-IVR makes it promising for treating complex molecular systems.

V. CONCLUDING REMARKS

In this paper, the forward–backward initial value representation (FB-IVR) has been used to study quantum coherence effects in the time-dependent probability distribution function of an anharmonic vibrational coordinate and its quenching when coupled to a thermal bath. These results should provide a reasonable indication of the level of quantum coherence/interference, and to what extent it is quenched by an environment (e.g., a cluster, a liquid, a surface, a protein, etc.). Since the FB-IVR is capable of describing these quantum effects, it thus provides a reliable way of knowing when such effects are important (or when they are not).

If the coupling between the vibrational coordinate and the bath is zero, quantum coherence persists for infinitely long time. The FB-IVR accurately reproduces the detailed coherent structure, even for a reasonably long time. The LSC-IVR/classical Wigner model, however, is only accurate for short time dynamics (when coherence has not emerged) and is unable to describe true quantum coherence. On the other hand, a single trajectory approximation, where the semiclassical phase space average is replaced by one average trajectory, exaggerates the coherence and also leads to incorrect results. Therefore, caution must be taken in applying various approximations to the study of the vibrational relaxation process if its coupling with the environment is weak.³⁶

When the vibrational coordinate is coupled to a thermal bath, its dynamics is influenced by the environment and the quantum coherence is quenched at longer time. This is the well-known decoherence effect in a complex molecular system, the extent of which depends on several parameters. In this paper, coherent to incoherent transitions are observed with the increase of both the system–bath coupling strength and the bath temperature. At room temperature and a reasonably large coupling strength, almost all the coherent structure is quenched by the bath. In this regime classical mechanics is a good approximation.

The FB-IVR approach provides an accurate yet practical description of quantum effects for complex molecular systems. For the present problem, 50 000–100 000 trajectories are usually sufficient to achieve numerical convergence, and this number is rather insensitive to the number of degrees of freedom. Though in some regimes classical mechanics is

also satisfactory, one does not have *a priori* information of when this is the case. The FB-IVR can be applied to determine if a certain problem meets such criteria, and thus serves as a more reliable tool in dynamical studies of large systems.

ACKNOWLEDGMENTS

This work was supported by the Director, Office of Science, Office of Basic Energy Sciences, Chemical Sciences Division of the U.S. Department of Energy under Contract No. DE-AC03-76SF00098, and by National Science Foundation Grant CHE 97-32758. M.T. gratefully acknowledges a Feodor–Lynen fellowship of the Alexander von Humboldt Foundation. R.G. thanks the ‘‘Fundación Ramón Areces’’ of Spain for a post-doctoral fellowship. X.G. acknowledges the Spanish MEC for a ‘‘Formación y Movilidad de Profesorado Universitario’’ fellowship.

¹For reviews, see W. H. Miller, *Faraday Discuss.* **110**, 1 (1998).

²W. H. Miller, *J. Chem. Phys.* **53**, 3578 (1970).

³M. F. Herman and E. Kluk, *Chem. Phys.* **91**, 27 (1984); E. Kluk, M. F. Herman, and H. L. Davis, *J. Chem. Phys.* **84**, 326 (1986); M. F. Herman, *Chem. Phys. Lett.* **275**, 445 (1997); B. E. Guerin and M. F. Herman, *ibid.* **286**, 361 (1998).

⁴E. J. Heller, *J. Chem. Phys.* **94**, 2723 (1991); **95**, 9431 (1991); F. Grossman and E. J. Heller, *Chem. Phys. Lett.* **241**, 45 (1995).

⁵K. G. Kay, *J. Chem. Phys.* **100**, 4377 (1994); **100**, 4432 (1994); **101**, 2250 (1994).

⁶G. Campolieti and P. Brumer, *Phys. Rev. A* **50**, 997 (1994); D. Provost and P. Brumer, *Phys. Rev. Lett.* **74**, 250 (1995); G. Campolieti and P. Brumer, *J. Chem. Phys.* **109**, 2999 (1998); B. R. McQuarrie and P. Brumer, *Chem. Phys. Lett.* **319**, 27 (2000).

⁷S. Garashchuk and D. J. Tannor, *Chem. Phys. Lett.* **262**, 477 (1996); S. Garashchuk, F. Grossmann, and D. J. Tannor, *J. Chem. Soc., Faraday Trans.* **93**, 781 (1997); S. Garashchuk and D. J. Tannor, *J. Chem. Phys.* **109**, 3028 (1998); D. J. Tannor and S. Garashchuk, *Annu. Rev. Phys. Chem.* **51**, 000 (2000).

⁸A. R. Walton and D. E. Manolopoulos, *Mol. Phys.* **87**, 961 (1996); A. R. Walton and D. E. Manolopoulos, *Chem. Phys. Lett.* **244**, 448 (1995); M. L. Brewer, J. S. Hulme, and D. E. Manolopoulos, *J. Chem. Phys.* **106**, 4832 (1997).

⁹W. H. Miller, *J. Chem. Phys.* **95**, 9428 (1991); B. W. Spath and W. H. Miller, *ibid.* **104**, 95 (1996); X. Sun and W. H. Miller, *ibid.* **106**, 916 (1997); **106**, 6346 (1997); **108**, 8870 (1998); V. S. Batista, M. T. Zanni, B. J. Greenblatt, D. M. Neumark, and W. H. Miller, *ibid.* **110**, 3736 (1999); V. Guallar, V. S. Batista, and W. H. Miller, *ibid.* **110**, 9922 (1999); D. E. Skinner and W. H. Miller, *Chem. Phys. Lett.* **300**, 20 (1999); E. A. Coronado, V. S. Batista, and W. H. Miller, *J. Chem. Phys.* **112**, 5566 (2000); M. Thoss, W. H. Miller, and G. Stock, *ibid.* **112**, 10282 (2000).

¹⁰D. V. Shalashilin and B. Jackson, *Chem. Phys. Lett.* **291**, 143 (1998); **318**, 305 (2000).

¹¹G. Stock and M. Thoss, *Phys. Rev. Lett.* **78**, 578 (1997); M. Thoss and G. Stock, *Phys. Rev. A* **59**, 64 (1999).

¹²G. van de Sand and J.-M. Rost, *Phys. Rev. Lett.* **83**, 524 (1999).

¹³F. Grossmann, *Phys. Rev. A* **60**, 1791 (1999).

¹⁴B. J. Berne and G. D. Harp, *Adv. Chem. Phys.* **17**, 63 (1970).

¹⁵H. Wang, X. Sun, and W. H. Miller, *J. Chem. Phys.* **108**, 9726 (1998).

¹⁶E. J. Heller, *J. Chem. Phys.* **65**, 1289 (1976); R. C. Brown and E. J. Heller, *ibid.* **75**, 186 (1981); H. W. Lee and M. O. Scully, *ibid.* **73**, 2238 (1980); J. S. Cao and G. A. Voth, *ibid.* **104**, 273 (1996); R. E. Cline, Jr. and P. G. Wolynes, *ibid.* **88**, 4334 (1988); V. Khidekel, V. Chernyak, and S. Mukamel, in *Femtochemistry: Ultrafast Chemical and Physical Processes in Molecular Systems*, edited by Majed Chergui (World Scientific, Singapore, 1996), p. 507.

¹⁷X. Sun, H. Wang, and W. H. Miller, *J. Chem. Phys.* **109**, 7064 (1998); H. Wang, X. Song, D. Chandler, and W. H. Miller, *ibid.* **110**, 4828 (1999).

¹⁸E. Pollak and J. L. Liao, *J. Chem. Phys.* **108**, 2733 (1998); J. Shao, J. L. Liao, and E. Pollak, *ibid.* **108**, 9711 (1998).

¹⁹W. H. Miller, *J. Chem. Phys.* **61**, 1823 (1974); W. H. Miller, S. D. Schwartz, and J. W. Tromp, *ibid.* **79**, 4889 (1983).

- ²⁰X. Sun, H. Wang, and W. H. Miller, *J. Chem. Phys.* **109**, 4190 (1998).
- ²¹X. Sun and W. H. Miller, *J. Chem. Phys.* **110**, 6635 (1999); also see Ref. 1.
- ²²N. Makri and K. Thompson, *Chem. Phys. Lett.* **291**, 101 (1998); K. Thompson and N. Makri, *Phys. Rev. E* **59**, R4729 (1999).
- ²³H. Wang, M. Thoss, and W. H. Miller, *J. Chem. Phys.* **112**, 47 (2000).
- ²⁴R. Gelabert, X. Giménez, M. Thoss, H. Wang, and W. H. Miller, *J. Phys. Chem. A* **104**, 10321 (2000); R. Gelabert, X. Giménez, M. Thoss, H. Wang, and W. H. Miller, *J. Chem. Phys.* **114**, 2572 (2001), following paper.
- ²⁵T. Elsaesser and W. Kaiser, *Annu. Rev. Phys. Chem.* **42**, 83 (1991).
- ²⁶J. C. Owrutsky, D. Raftery, and R. M. Hochstrasser, *Annu. Rev. Phys. Chem.* **45**, 519 (1994).
- ²⁷T. Uzer, *Phys. Rep.* **199**, 124 (1991).
- ²⁸D. J. Nesbitt and R. W. Field, *J. Phys. Chem.* **100**, 12735 (1996).
- ²⁹C. Lienau and A. H. Zewail, *J. Phys. Chem.* **100**, 18629 (1996).
- ³⁰B. J. Greenblatt, M. T. Zanni, and D. M. Neumark, *Faraday Discuss.* **108**, 101 (1997).
- ³¹C. J. Bardeen, J. Che, K. R. Wilson, V. V. Yakovlev, V. A. Apkarian, C. C. Martens, R. Zadoyan, B. Kohler, and M. Messina, *J. Chem. Phys.* **106**, 8486 (1997).
- ³²P. K. Walhout, J. C. Alfano, K. A. M. Thakur, and P. F. Barbara, *J. Phys. Chem.* **99**, 7568 (1995).
- ³³J.-Y. Fang and C. C. Martens, *J. Chem. Phys.* **105**, 9072 (1996).
- ³⁴A. J. Leggett, S. Chakravarty, A. T. Dorsey, M. P. Fisher, A. Garg, and W. Zwerger, *Rev. Mod. Phys.* **59**, 1 (1987).
- ³⁵K. Husimi, *Proc. Phys. Math. Soc. Jpn.* **22**, 264 (1940).
- ³⁶For discussions on this topic, see, for example, S. A. Egorov, E. Rabani, and B. J. Berne, *J. Phys. Chem. B* **103**, 10978 (1999); S. A. Egorov, K. F. Everitt, and J. L. Skinner, *J. Phys. Chem. A* **103**, 9494 (1999).